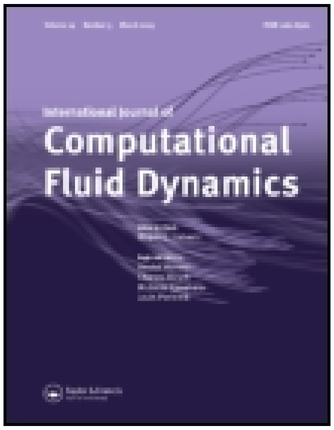

International Journal of Computational Fluid Dynamics
Publication details, including instructions for authors and subscription information:
http://www.tandfonline.com/loi/gcfd20

Non-oscillatory central-upwind scheme for hyperbolic conservation laws

Yousef Hashem Zahran [a]
[a] Physics and Mathematics Department , Faculty of Engineering , Port Said, Egypt
Published online: 25 May 2007.

International Journal of Computational Fluid Dynamics, Vol. 21, No. 1, January 2007, 11–19

Non-oscillatory central-upwind scheme for hyperbolic conservation laws

YOUSEF HASHEM ZAHRAN*

Physics and Mathematics Department, Faculty of Engineering, Port Said, Egypt

(Received December 2006; in final form 20 March 2007)

We introduce a new fourth order, semi-discrete, central-upwind scheme for solving systems of hyperbolic conservation laws. The scheme is a combination of a fourth order non-oscillatory reconstruction, a semi-discrete central-upwind numerical flux and the third order TVD Runge-Kutta method. Numerical results suggest that the new scheme achieves a uniformly high order accuracy for smooth solutions and produces non-oscillatory profiles for discontinuities. This is especially so for long time evolution problems. The scheme combines the simplicity of the central schemes and accuracy of the upwind schemes. The advantages of the new scheme will be fully realized when solving various examples.

Keywords: Central scheme; Upwind scheme; Runge-Kutta methods; Non-oscillatory schemes; Conservation laws; Semi-discrete schemes; Euler equations

1. Introduction

We are concerned with improved very high order methods for solving hyperbolic conservation laws. Analytic solutions are available only in very few special cases and numerical methods must be used in practical applications. Developing such methods is formidable since solutions can contain complex smooth structures interspersed with discontinuities. A successful numerical method should resolve discontinuities with correct positions and sharp non-oscillatory profiles and retain high order of accuracy in smooth regions.

There are two main types of schemes: upwind schemes and central schemes. Upwind schemes utilize information on local wave propagation explicitly. Godunov first introduced the idea of using the exact solution of the local Riemann problem (RP) to compute the upwind flux. The use of the RP incorporates the physics of wave propagation into the numerical method and leads to more accurate results as compared to central flux. On the other hand, central schemes do not use Riemann solvers and characteristic decomposition, which make them simple, efficient and applicable to very complex equations but also very diffusive as compared to upwind schemes.

Central-upwind schemes, introduced in Kurganov *et al.* (2001), are semi-discrete variants of central methods which have improved efficiency and less dissipation than fully discrete central methods.

Many of the high order methods used an interpolating polynomial that reconstructs the point-values of the solution in terms of the cell averages. Second order schemes require a piecewise linear reconstruction (Nessyahu and Tadmor 1990). Third order schemes employ a quadratic piecewise approximation (Kurganov and Levy 2000, Kurganov and Petrova 2001), and one of the possibilities is to use the essentially non-oscillatory (ENO) reconstruction (Harten *et al.* 1987). The weighted ENO interpolants are proposed in Jiang and Shu (1996) and Balsara and Shu (2000). The ENO-type approach employs smoothness indicators. They require a certain *a priori* information about the solution, which may be unavailable and then spurious oscillations or extrema smearing of discontinuities may appear.

One-dimensional fourth order non-oscillatory piecewise reconstruction, which do not require the use of smoothness indicators, was proposed in Balagur and Conde (2005).

In this paper, we propose a new fourth order, semi-discrete, central-upwind scheme for solving one-dimensional systems of hyperbolic conservation laws. This scheme combines a fourth order non-oscillatory reconstruction (Balagur and Conde 2005), a semi-discrete central-upwind numerical flux (Kurganov *et al.* 2001) and the three stage third order TVD Runge-Kutta method

*Email: yousef_hashem_zahran@yahoo.com

International Journal of Computational Fluid Dynamics
ISSN 1061-8562 print/ISSN 1029-0257 online © 2007 Taylor & Francis
http://www.tandf.co.uk/journals
DOI: 10.1080/10618560701371458

(Gottlieb *et al.* 2001). For the fourth order reconstruction (Balagur and Conde 2005), we used the more general form of the reconstruction presented in Kurganov and Petrova (2001) to guarantee the non-oscillatory property. Numerical results suggest that the new scheme proposed here improve upon the original fourth order scheme (Balagur and Conde 2005) in terms of better convergence, higher overall accuracy and better resolution of discontinuities, due to smaller amount of the numerical dissipation. This is especially so for long time evolution problems

The paper is organized as follows. In section 2, we introduce our new fourth order central-upwind scheme, summarizing the fourth order reconstruction (Balagur and Conde 2005) in section 2.1. In section 2.2, we summarize the derivation of the central-upwind flux (Kurganov *et al.* 2001). Third order TVD Runge-Kutta method (Gottlieb *et al.* 2001) of time discretization is briefly reviewed in section 2.3. Section 3 presents the results of number of numerical tests of our method.

2. The numerical scheme

In this section, we review the components we use to construct our fourth order central-upwind scheme for hyperbolic systems in conservative form

$$u_t + [f(u)]_x = 0 \tag{2.1}$$

along with initial and boundary conditions. Here, $u(x, t)$ is the vector of unknown conservative variables and $f(u)$ is the physical flux vector. Throughout this paper, we consider only uniform grids and use the following notation - let

$$x_j = j\Delta x, x_{j\pm(1/2)} = x_j \pm (1/2)\Delta x, \quad t^n = n\Delta t, \quad u_j^n = u(x_j, t^n)$$

and the cell $I_j = [x_{j-(1/2)}, x_{j+(1/2)}]$, where Δx and Δt are small spatial and time scales. Consider a control volume in x-space $[x_{j-(1/2)}, x_{j+(1/2)}]$. Integrating (2.1) with respect to x over the volume and keeping the time variable continuous we obtain the semi-discrete finite volume scheme which is in fact a system of ordinary differential equations (ODEs)

$$\frac{\mathrm{d}}{\mathrm{d}t}u_j(t) = -\frac{1}{\Delta x}\{F_{j+(1/2)} - F_{j-(1/2)}\} = L_j(u) \tag{2.2}$$

where $u_j(t)$ is the space average of the solution in the cell I_j at time t and $F_{j+(1/2)}$ is the numerical flux at $x = x_{j+(1/2)}$ and time t

$$\begin{aligned} u_j(t) &= \frac{1}{\Delta x}\int_{x_{j-(1/2)}}^{x_{j+(1/2)}} u(x,t)\mathrm{d}x, \\ F_{j+(1/2)} &= F(u_{j+(1/2)}(t)). \end{aligned} \tag{2.3}$$

The steps to follow in the implementation of the numerical scheme (2.2) can be described as follows:

(i) The first step in the derivation of the approximate solution is to generate a piecewise polynomial reconstruction from the cell averages. Such a global reconstruction is defined as

$$u(x, t^n) = P_j^n(x), \quad x_{j-(1/2)} \le x \le x_{j+(1/2)} \tag{2.4}$$

where $P_j^n(x)$ are polynomial of a suitable degree.

In each cell I_j the reconstruction should be conservative, formally r-th order accurate and non-oscillatory. As a result, at each cell interface $x_{j+(1/2)}$ between cells j and $j+1$ the reconstruction produces two different values of the vector of conservative u, namely the left extrapolated value $u^-_{j+(1/2)} = P_j(x_{j+(1/2)})$ and the right extrapolated value $u^+_{j+(1/2)} = P_{j+1}(x_{j+(1/2)})$.

In section 2.1, we will give a brief description of the fourth order non-oscillatory reconstruction from Balagur and Conde (2005), which will be used in our scheme.

(ii) The second step is to evaluate the numerical flux at the cell boundary $x_{j+(1/2)}$ as a monotone function of left and right extrapolated values $u^\pm_{j+(1/2)}$:

$$F_{j+(1/2)} = F(u_{j+(1/2)}(t)) = F_{j+(1/2)}\left(u^-_{j+(1/2)}, u^+_{j+(1/2)}\right). \tag{2.5}$$

Here, we use the central-upwind flux, introduced in Kurganov *et al.* (2001). The flux is based on the use of more precise information about the local speeds of propagation. The main advantages of this flux are high resolution, due to smaller amount of the numerical dissipation, the simplicity and no Riemann solvers and characteristic decomposition involved. In section 2.2, we review the derivation of this flux.

(iii) The semi-discrete scheme (2.2) is a system of time dependent ODEs, which can be solved by any stable ODE solver which retain the spatial accuracy of the semi-discrete scheme. Here, we use the third order TVD Runge-Kutta method (Gottlieb *et al.* 2001). We will present this method in section 2.3.

2.1 Non-oscillatory piecewise polynomial reconstruction

As we have already mentioned, one of the three building blocks of the numerical scheme (2.2) is a piecewise polynomial reconstruction. A fourth order non-oscillatory reconstruction was proposed in Balagur and Conde (2005). Here, we give a brief description of this reconstruction which will be used in our scheme (2.2).

Firstly, for a scalar function $u(x)$, we consider the degree three reconstruction

$$\begin{aligned} q_j(x) = u_j^n &- \frac{1}{24}[u_{j-1} - 2u_j + u_{j+1}] \\ &+ \frac{1}{8}[u_{j-1} - u_{j+1} + 10d_j^n]\left(\frac{x-x_j}{\Delta x}\right) \\ &+ \frac{1}{2}[u_{j-1} - 2u_j + u_{j+1}]\left(\frac{x-x_j}{\Delta x}\right)^2 \\ &+ \frac{1}{2}[-u_{j-1} + u_{j+1} - 2d_j^n]\left(\frac{x-x_j}{\Delta x}\right)^3 \end{aligned} \tag{2.6}$$

which is conservative and fourth order accurate. Here, d_j^n is a slope function.

The reconstruction (2.6) should satisfy the shape preserving and non-oscillatory properties.

To make (2.6) satisfy the preserving properties we have to define a procedure that adequately defines the slopes d_j^n. For this, we use the notation

$$\begin{aligned}
\mathrm{d}S_j^n &= \frac{2}{3}u_{j+1} - \frac{2}{3}u_{j-1} - \frac{1}{12}u_{j+2} + \frac{1}{12}u_{j-2},\\
WC_j^n &= u_{j+1} - u_{j-1},\quad WR_j^n = u_{j+1} - u_j,\\
WC2_j^n &= u_{j+2} - u_{j-2},\quad \mathrm{d}S1_j^n = \frac{WC_j^n}{10},\\
\mathrm{d}S2_j^n &= \frac{1}{2}(WC_j^n - 4WR_j^n)\\
\mathrm{d}S3_j^n &= \frac{1}{2}(4WR_j^n - 3WC_j^n),\quad S_j^n = \mathrm{sgn}(WC_j^n),\\
C1 &= \frac{\sqrt{15}}{15},\quad C2 = \frac{15-\sqrt{15}}{28}
\end{aligned}$$

THEOREM. The reconstructions (2.6) satisfies the shape preserving properties if d_j^n verifies:

(A1) If $S_j^n = 0$, then $d_j^n = 0$,
(A2) If $S_j^n \neq 0$ and $(2S_j^n.WC_j^n \geq S_j^n.WC2_j^n)$, then $d_j^n = \mathrm{d}S_j^n$
(A3) If $S_j^n \neq 0$ and $(2S_j^n.WC_j^n < S_j^n.WC2_j^n)$, then the following hold:
  (A3.1) If $u_j^n = ((u_{j+1}^n + u_{j-1}^n)/2)$ we define

$$d_j^n = \begin{cases} \mathrm{Max}[\mathrm{d}S1_j^n, \mathrm{d}S_j^n], & \text{if } S_j^n > 0,\\ \mathrm{Min}[\mathrm{d}S1_j^n, \mathrm{d}S_j^n], & \text{if } S_j^n < 0,\end{cases}$$

  (A3.2) If $u_j^n \neq ((u_{j+1}^n + u_{j-1}^n)/2)$ then the following hold
    (A3.2.1) If $|WR_j^n - (1/2)WC_j^n| \geq (1/8)\,|WC2_j^n - 2WC_j^n|$, then

$$d_j^n = \begin{cases} \mathrm{Max}\left[\mathrm{d}S2_j^n, \mathrm{d}S3_j^n, \mathrm{d}S_j^n\right], & \text{if } S_j^n > 0,\\ \mathrm{Min}\left[\mathrm{d}S2_j^n, \mathrm{d}S3_j^n, \mathrm{d}S_j^n\right], & \text{if } S_j^n < 0,\end{cases}$$

    (A3.2.2) If $|WR_j^n - (1/2)WC_j^n| < (1/8)\,|WC2_j^n - 2WC_j^n|$, then

$$d_j^n = \begin{cases} WC_j^n - S_j^n.C1.\left|2WR_j^n - WC_j^n\right| & \text{if}.\left|\frac{WR_j^n}{WC_j^n} - \frac{1}{2}\right| \leq C2\\ \frac{WC_j^n}{2} & \text{if}.\left|\frac{WR_j^n}{WC_j^n} - \frac{1}{2}\right| > C2.\end{cases}$$

Proof. See (Balagur and Conde 2005). To obtain a non-oscillatory reconstruction (Balagur and Conde 2005) consider the modified piecewise reconstruction

$$P_j^n(x) = (1-\theta_j^n)u_j^n + \theta_j^n\ \ q_j^n(x) \quad 0 < \theta_j^n < 1. \tag{2.7}$$

Here, we use a more general form proposed in Kurganov and Petrova (2001) which is a combination of q_j^n and the piecewise linear L_j^n, namely

$$P_j^n(x) = (1-\theta_j^n)L_j^n + \theta_j^n\ \ q_j^n(x) \quad 0 < \theta_j^n < 1 \tag{2.8}$$

where

$$L_j^n(x) = u_j^n + w_j^n(x - x_j). \tag{2.9}$$

An appropriate choice of $\{\theta_j^n\}$ and $\{w_j^n\}$ guarantees the non-oscillatory property of the new piecewise reconstruction $P_j^n(x)$ (Kurganov and Petrova 2001). We take $\{\theta_j^n\}$ to be

$$\theta_j^n = \begin{cases} \mathrm{Min}\left(\frac{M_{j+(1/2)}^n - L_j^n(x_{j+(1/2)})}{M_j^n - L_j^n(x_{j+(1/2)})}, \frac{m_{j-(1/2)}^n - L_j^n(x_{j-(1/2)})}{m_j^n - L_j^n(x_{j-(1/2)})}, 1\right) & \\ \qquad\qquad \text{if } u_{j-1}^n < u_j^n < u_{j+1}^n, & \\ \mathrm{Min}\left(\frac{M_{j-(1/2)}^n - L_j^n(x_{j-(1/2)})}{M_j^n - L_j^n(x_{j-(1/2)})}, \frac{m_{j+(1/2)}^n - L_j^n(x_{j+(1/2)})}{m_j^n - L_j^n(x_{j+(1/2)})}, 1\right) & \\ \qquad\qquad \text{if } u_{j-1}^n > u_j^n > u_{j+1}^n, & \\ 1 \qquad\qquad \text{otherwise} & \end{cases} \tag{2.10}$$

where

$$M_j^n = \max\left\{q_j^n(x_{j+(1/2)}), q_j^n(x_{j-(1/2)})\right\} \text{ and}$$

$$m_j^n = \min\left\{q_j^n(x_{j+(1/2)}), q_j^n(x_{j-(1/2)})\right\}$$

and

$$\begin{aligned}
M_{j\pm(1/2)}^n &= \max\left\{\frac{1}{2}L_j^n(x_{j\pm(1/2)}) + L_{j\pm1}^n(x_{j\pm(1/2)}), q_{j\pm1}^n(x_{j\pm(1/2)})\right\},\\
m_{j\pm(1/2)}^n &= \min\left\{\frac{1}{2}L_j^n(x_{j\pm(1/2)}) + L_{j\pm1}^n(x_{j\pm(1/2)}),\ \ q_{j\pm1}^n(x_{j\pm(1/2)})\right\}
\end{aligned}$$

Here, we take w_j^n as following (Kurganov and Petrova 2001)

$$w_j^n = \min\ i\ \bmod\left\{\frac{u_j^n - u_{j-1}^n}{\Delta x}, \frac{u_{j+1}^n - u_j^n}{\Delta x}\right\}. \tag{2.11}$$

If one sets w_j^n to be zero, then (2.8)–(2.10) is reduced to the original reconstruction (Balagur and Conde 2005).

The reconstruction for the systems is carried out by component wise application of the scalar framework.

2.2 The central-upwind flux

In this section, we summarize the derivation of the central-upwind flux presented in Kurganov and Levy (2000) and Kurganov and Tadmor (2000).

We consider the one-dimensional system (2.1) of N strictly hyperbolic conservation laws. We start with a piecewise polynomial reconstruction (2.4) with possible discontinuities at the interface points $\{x_{j+(1/2)}\}$. These discontinuities propagate with right- and left-sided local speeds, which can be estimated by

$$a^+_{j+(1/2)} = \max_{v\in C(u^+_{j+(1/2)},u^-_{j+(1/2)})}\left\{\lambda_N\left(\frac{\partial f}{\partial u}(v)\right),0\right\},$$

$$a^-_{j+(1/2)} = \min_{v\in C(u^+_{j+(1/2)},u^-_{j+(1/2)})}\left\{\lambda_1\left(\frac{\partial f}{\partial u}(v)\right),0\right\}.$$

Here, $\lambda_1 < \cdots < \lambda_N$ denote the N eigenvalues of the Jacobian of F and $C(u^-_{j+(1/2)}, u^+_{j+(1/2)})$ is the curve in phase space connecting $u^-_{j+(1/2)}$ and $u^+_{j+(1/2)}$. These local speeds of propagation are used to determine intervals of averaging that contain the Riemann fans from the cell interfaces. An exact evolution of the reconstruction is followed by an intermediate piecewise polynomial reconstructions and finally projected back onto the original cells, providing the cell average at the next time step u_j^{n+1}. Further details can be found in Kurganov and Levy (2000). The semi-discrete central-upwind scheme presented in Kurganov *et al.* (2001) can be written as

$$\frac{\mathrm{d}}{\mathrm{d}t}u_j(t) = -\frac{1}{\Delta x}\{F_{j+(1/2)} - F_{j-(1/2)}\} = L_j(u). \tag{2.12}$$

The numerical flux in (2.12) is given by

$$F_{j+(1/2)} = \frac{a^+_{j+(1/2)} f\left(u^-_{j+(1/2)}\right) - a^-_{j+(1/2)} f\left(u^+_{j+(1/2)}\right)}{a^+_{j+(1/2)} - a^-_{j+(1/2)}} + \frac{a^+_{j+(1/2)}\, a^-_{j+(1/2)}}{a^+_{j+(1/2)} - a^-_{j+(1/2)}}\left[u^+_{j+(1/2)} - u^-_{j+(1/2)}\right]. \tag{2.13}$$

The accuracy of this scheme is determined by the accuracy of the reconstruction and the ODE solver.

2.3 Time discretization

The semi-discrete (2.2) is a system of time dependent ODEs, which can solved by any stable ODE solver which retain the spatial accuracy of the scheme. Here, we use the TVD Runge-Kutta method presented (Gottlieb *et al.* 2001).

These Runge-Kutta methods are used to solve a system of ODEs

$$\frac{\mathrm{d}u}{\mathrm{d}t} = L(u), \tag{2.14}$$

where $L(u)$ is an approximation to the derivative $(-f(u)_x)$ in the differential equation (2.1).

The optimal third order TVD Runge-Kutta method is given by

$$\begin{aligned} u^{(1)} &= u^n + \Delta t\ L(u^n) \\ u^{(2)} &= \frac{3}{4}u^n + \frac{1}{4}u^{(1)} + \frac{1}{4}\Delta t\ L(u^{(1)}) \\ u^{n+1} &= \frac{1}{3}u^n + \frac{2}{3}u^{(2)} + \frac{2}{3}\Delta t\ L(u^{(2)}). \end{aligned} \tag{2.15}$$

In Gottlieb *et al.* (2001), it has been shown that, even with a very nice second order TVD spatial discretization, if the time discretization is by a non-TVD but linearly stable Runge-Kutta method, the result may be oscillatory. Thus it would always be safer to use TVD Runge-Kutta methods for hyperbolic problems.

3. Numerical results

In this section, we test our new scheme, proposed here, on various examples and compare the numerical results with the original fourth order scheme (Balagur and Conde 2005). The new scheme (2.2) differs from the original scheme (Balagur and Conde 2005) in that it is a semi-discrete central-upwind scheme in which we use the central-upwind flux (2.13), fourth order reconstruction (2.8) and the time dicretization (2.15). For all calculations we use the CFL condition $\Delta t = 0.8(\Delta x/|\lambda_j|)$, where λ_j denote the eigenvalues of the Jacobian of the flux $f(x,\, t)$ evaluated at x_j. An important issue is the choice of test problems. We would like to emphasise here the importance of using really long time evolution problems with solutions consisting of discontinuities and smooth parts.

We compare the following schemes:

1. F4 it is the original fourth order scheme (Balagur and Conde 2005), and
2. FCW it is the new scheme (2.2) presented here.

3.1 Scalar equations

First, we solve a test problem with a very smooth solution in order to see how the central-upwind flux influences the convergence property of the scheme.

3.1.1 Example 1. Smooth solution. We solve the equation

$$u_t + u_x = 0, \quad x \in [-1, 1] \tag{3.1}$$

subjected to periodic initial data

$$u(x, 0) = \sin^4(\pi x). \tag{3.2}$$

We use output times $t = 1$ and very long time $t = 1000$. Tables 1 and 2 show grid convergence rates and errors in L^1 and L^∞ norms for the space variable. From table 1

Table 1. At $t = 1$.

	F4		FCW		F4		FCW	
N	L^1 error	L^1 order	L^1 error	L^1 order	L^∞ error	L^∞ order	L^∞ error	L^∞ order
40	3.071×10^{-5}		1.134×10^{-5}		2.498×10^{-5}		2.466×10^{-5}	
80	1.746×10^{-6}	4.14	5.553×10^{-7}	4.35	1.396×10^{-6}	4.16	1.201×10^{-6}	4.36
160	1.056×10^{-7}	4.05	2.919×10^{-8}	4.25	8.375×10^{-8}	4.06	6.567×10^{-8}	4.19
320	6.529×10^{-9}	4.02	1.562×10^{-9}	4.22	5.152×10^{-9}	4.02	3.338×10^{-9}	4.30

($t = 1$), we note that the scheme FCW is more accurate than F4 scheme. Moreover, the magnitudes of the errors of FCW are much smaller than of F4 scheme, even on coarsest mesh. For long time $t = 1000$ (table 2) FCW scheme is seen to converge much better than F4 scheme. We observe that the F4 scheme converges with second order of accuracy while the FCW converges to third order of accuracy.

3.1.2 Example 2. Solution containing discontinuities. We now consider the equation (3.1) with the initial condition (Balagur and Conde 2005)

$$u(x,0)=\begin{cases} \frac{1}{6}[G(x,z-\delta)+G(x,z+\delta)+4G(x,z)], & -0.8\le x\le -0.6 \\ 1, & -0.4\le x\le -0.2 \\ 1-|10(x-0.1)| & 0\le x\le 0.2 \\ \frac{1}{6}[F(x,a-\delta)+F(x,a+\delta)+4F(x,a)], & 0.4\le x\le 0.6 \\ 0, & \text{otherwise} \end{cases} \tag{3.3}$$

with periodic boundary condition on $[-1,1]$, where $G(x,z)=\exp(-\beta(x-z)^2)$, $F(x,a)=\{\max(1-\alpha^2(x-a)^2\}^{1/2}$. The constants are taken as $a=0.5$, $z=-0.7$, $\delta=0.005, \alpha=10$ and $\beta=(\log 2)/36\delta^2$.
This initial condition consists of several shapes which are difficult for numerical methods to resolve correctly. Some of these shapes are not smooth and the other are smooth but very sharp.

Figure 1 shows the numerical results at $t = 20$ obtained by FCW scheme with mesh size of 200 cells. The exact solution is shown by solid line and numerical solution shown by symbols. Comparing the results in figure 1 and figure 4.1 in Balagur and Conde (2005), we notice that the accuracy of FCW scheme is overall higher than that of F4 scheme. In particular, FCW provides better resolution of the discontinuous square pulse. We also note that the resolution of the left peak in FCW scheme is more sharp than F4 scheme.

To show the efficiency of the scheme we compute the solution at very long time $t = 2000$. Figures 2 and 3 depict graphical results of F4 and FCW schemes, respectively. We observe that the F4 scheme produces unacceptable results while the FCW scheme produces more accurate results for all parts of the solution, including the square pulse. This means that the use of central-upwind flux improves the accuracy and convergence properties of the scheme.

3.2 Systems of equations

In this section, we assess the performance of the new scheme for the system of Euler equations of gas dynamics

$$\text{where } U = (\rho, \rho u, E)^T \text{ and } F(U) = (\rho u, \rho u^2 + P, u(E + P))^T \tag{3.4}$$

where ρ is the density, u is the velocity, P is the pressure, $E = \rho e + (1/2)\rho u^2$ is the total energy, sum of internal energy and kinetic energy and e is the specific internal energy and γ is the ratio of specific heats.

3.2.1 Example 3. Shock reflection problem. We consider the test problem concerning shock reflection in one dimension $0 \le x \le 1$, governed by Euler equations of monatomic gas $\gamma = 5/3$ with initial data (Glaiter 1988):

$$\rho = \rho_0,\ \ u = -u_0\ \ e = e_0.$$

Table 2. At $t = 1000$.

	F4		FCW		F4		FCW	
N	L^1 error	L^1 order	L^1 error	L^1 order	L^∞ error	L^∞ order	L^∞ error	L^∞ order
40	5.451×10^{-3}		1.457×10^{-5}		7.681×10^{-3}		1.756×10^{-3}	
80	1.555×10^{-3}	1.81	1.608×10^{-4}	3.17	2.158×10^{-3}	1.83	1.935×10^{-4}	3.18
160	3.921×10^{-4}	1.99	2.134×10^{-5}	2.91	5.493×10^{-4}	1.97	2.752×10^{-5}	2.81
320	9.315×10^{-5}	2.07	2.669×10^{-6}	3.00	1.303×10^{-4}	2.08	3.353×10^{-6}	3.04

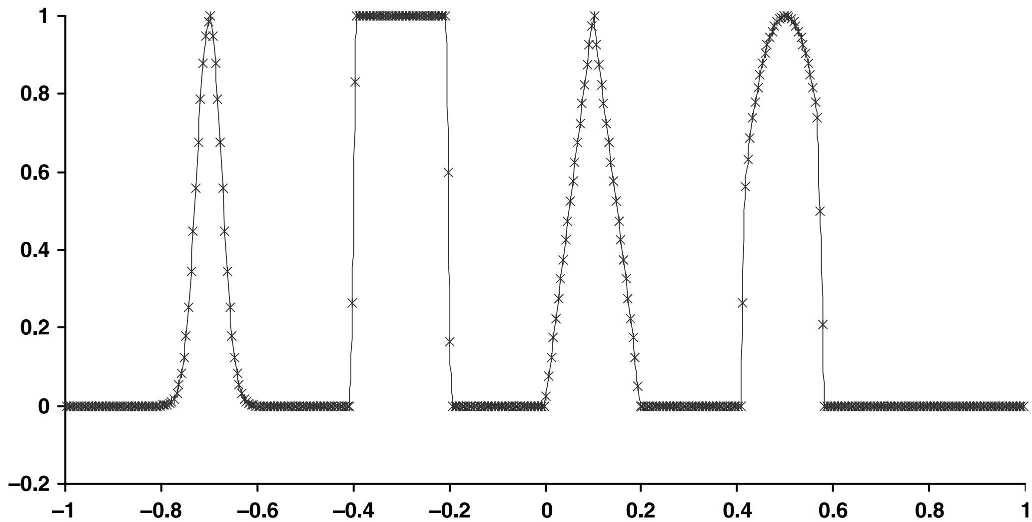

Figure 1. Solution of example 2 at $t = 20$ using FCW scheme.

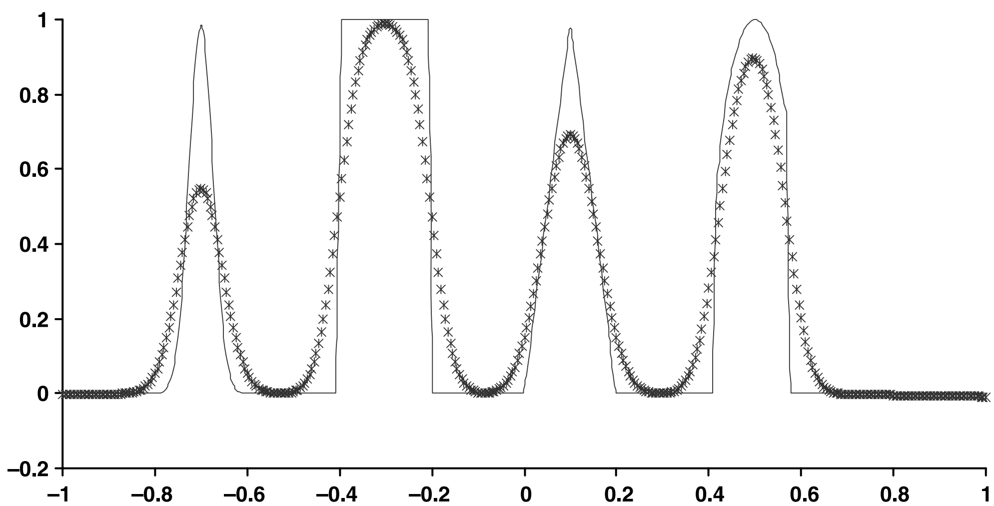

Figure 2. Solution of example 2 at $t = 2000$ using F4 scheme.

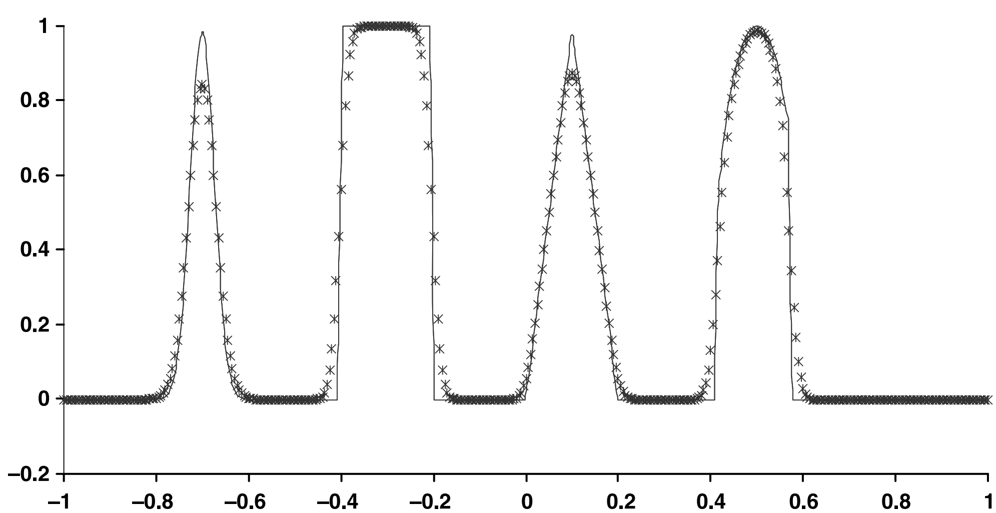

Figure 3. Solution of example 2 at $t = 2000$ using FCW scheme.

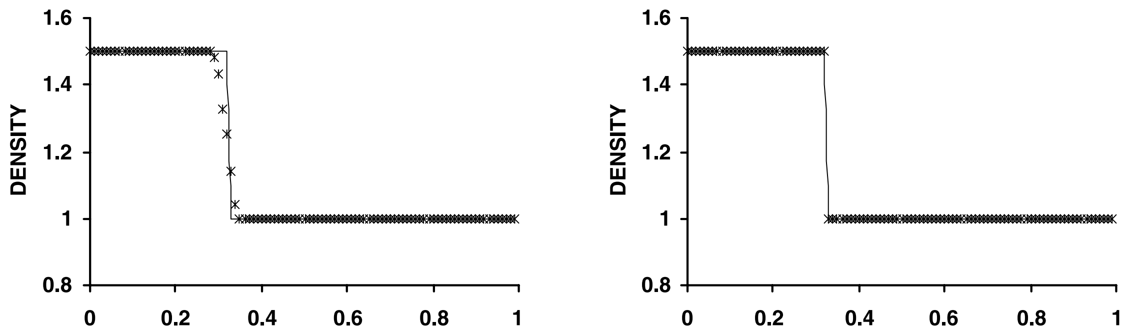

Figure 4. Solution of example 3 at $t = 0.15$ using F4 (left) and FCW (right).

This represents a gas of constant density and pressure moving towards $x = 0$. The boundary $x = 0$ is a rigid wall and exact solution describes shock reflection from the wall. The gas is brought to rest at $x = 0$ and

$$\rho_0 = 1, \ \ u_0 = 1, \ \ P_0 = 3 \tag{3.5}$$

$e(x, t)$ is chosen such that the pressure jump across the shock equals 2, i.e. $e_0 = 4.5$.

Figure 4 illustrates the results, at $t = 0.15$ and mesh size of 100 cells, for the F4 and FCW schemes, respectively. We observe that the FCW scheme resolves the discontinuity exactly while F4 scheme smears the discontinuity. This due to the choice of central-upwind flux in FCW scheme.

3.2.2 Example 4. Shock tube problem. We solve the shock tube problem (Sod 1987) for Euler equations (3.4) with $\gamma = 1.4$ and initial data consists of two states, left (L) and right (R)

$$(\rho_\mathrm{L}, u_\mathrm{L}, P_\mathrm{L}) = (1, 0, 1) \ \text{ and } \ (\rho_\mathrm{R}, u_\mathrm{R}, P_\mathrm{R}) = (0.125, 0, 0.1) \tag{3.6}$$

separated by a discontinuity at $x = 0.5$. The computational domain is taken as the unit interval [0,1] divided into 100 cells.

Figure 5 shows the results obtained by FCW scheme at $t = 0.16$. Comparing this results with figure (4.5) in Balagur and Conde (2005), we notice that the FCW is more accurate and economic since in Balagur and Conde (2005) CFL was taken as $\Delta t = 0.1\Delta x$ (with 200 cells) while here we take $\Delta t = 0.8\Delta x$ (with 100 cells) which save more time.

We notice also that the solution by FCW is almost indistinguishable from the exact solution.

3.2.3 Example 5. Shock/turbulence interaction problem. To show the advantages of our method we solve a problem containing both shock and complex smooth region structures. A typical example for this is the problem of shock interaction with entropy waves (Qiu and Shu 2002). We solve the Euler equations (3.4) with initial data defined on $[-5, 5]$

$$\begin{aligned}(\rho_\mathrm{L}, u_\mathrm{L}, P_\mathrm{L}) &= (3.857143, 2.629369, 10.3333), \ \text{for } x < -4\\ (\rho_\mathrm{R}, u_\mathrm{R}, P_\mathrm{R}) &= (1 + 0.2\sin 5x, 0, 1), \ \text{for } x > -4\end{aligned} \tag{3.7}$$

and $\gamma = 1.4$ which consists of a right-facing shock wave of Mach number 3 running into a high frequency density perturbation. The flow contains physical oscillations which have to be resolved by the numerical method. We compute the solution at $t = 1.8$. Figures 6 and 7 show the computed density by F4 and FCW schemes against the reference solution, which is a converged solution

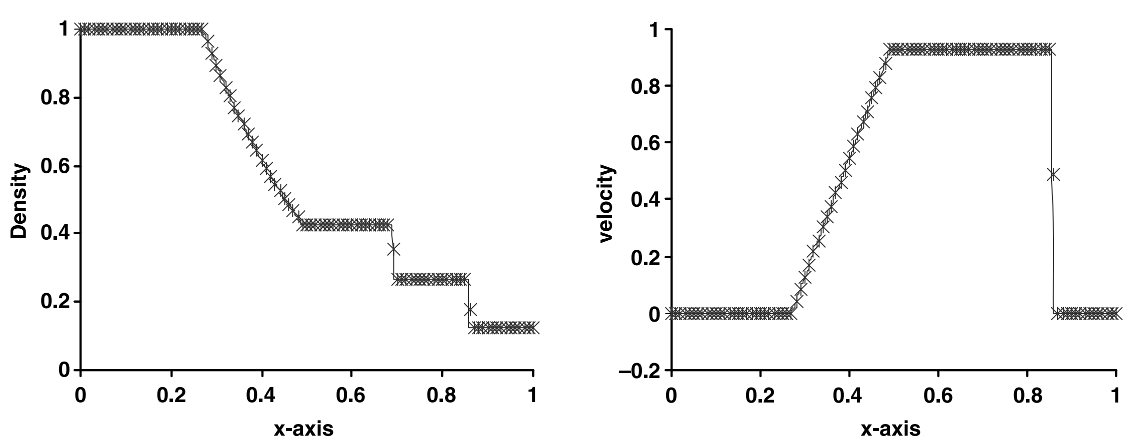

Figure 5. Solution of example 4 at $t = 0.16$ using FCW scheme.

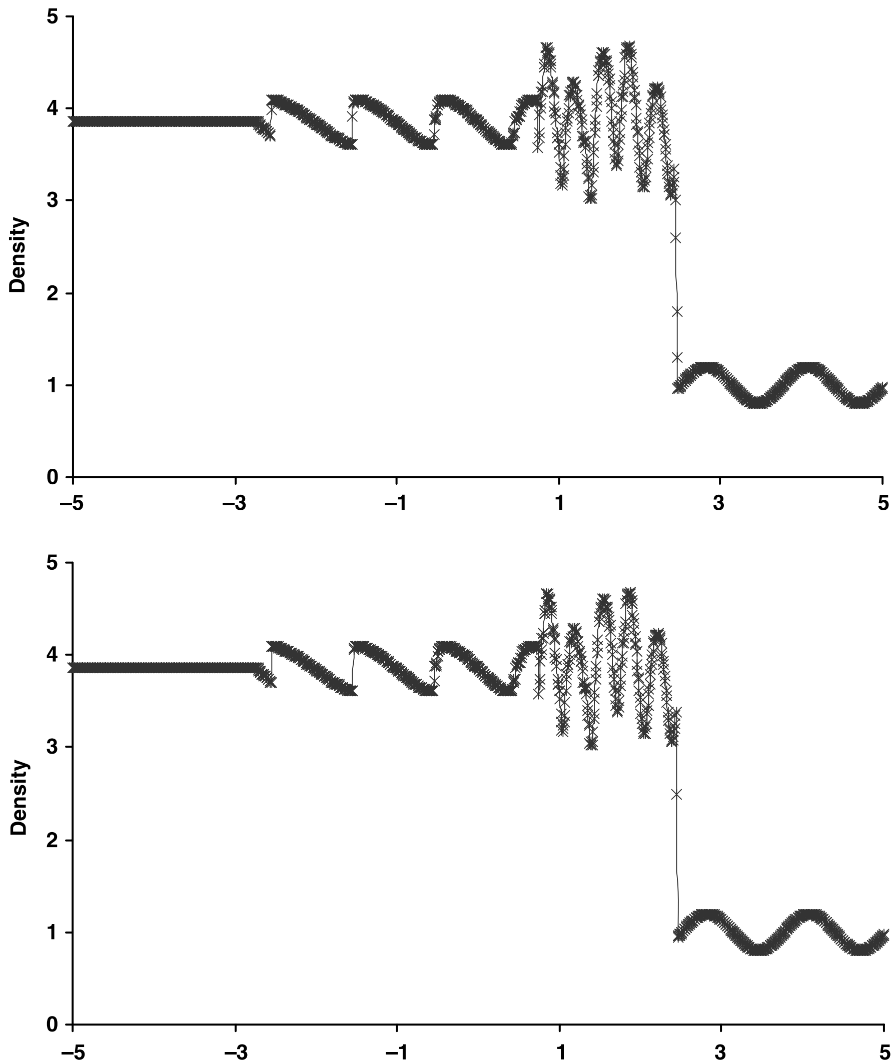

Figure 6. Solution of example 5 at $t = 1.8$ using F4 (up) and FCW (down).

computed by the fifth order finite difference WENO scheme (Qiu and Shu 2002) with 2000 grid points. Here, we use 200 grid points only and the time step $\Delta t = 0.8\Delta x$. From the figures, we observe the clear improvements in accuracy as we move from F4 to FCW scheme. Note that the undisturbed region ahead of the shock wave is well resolved by FCW scheme which produces a solution that is very close to the reference solution.

4. Extension to multidimensional problems

The present scheme can be applied to multidimensional problems by means of space operator splitting. As an example we consider the two-dimensional, Euler equations

$$U_t + [F(U)]_x + [G(U)]_y = 0 \tag{4.1}$$

where $U = (\rho, \rho u, \rho v, E)^T$, $F(U) = (\rho u, P + \rho u^2, \rho uv, u(P+E))^T$, $G(U) = (\rho v, \rho uv, P + \rho v^2, v(P+E))^T$. There are several versions of space splitting. Here, we take the simplest one, whereby the two-dimensional problem (4.1) is replaced by the sequence of two one-dimensional problems

$$U_t + [F(U)]_x = 0 \tag{4.2a}$$

$$U_t + [G(U)]_y = 0. \tag{4.2b}$$

If the data U^n at time level n for problem (4.1) are given, the solution U^{n+1} at time level $n+1$ is obtained in the following two steps:

(a) solve equation (4.2a) with data U^n to obtain an intermediate solution $\bar{U}^{n+1}$ (x-sweep); and
(b) solve equation (4.2b) with data $\bar{U}^{n+1}$ to obtain the complete solution U^{n+1} (y-sweep).

For three-dimensional problems there is an extra z-sweep.

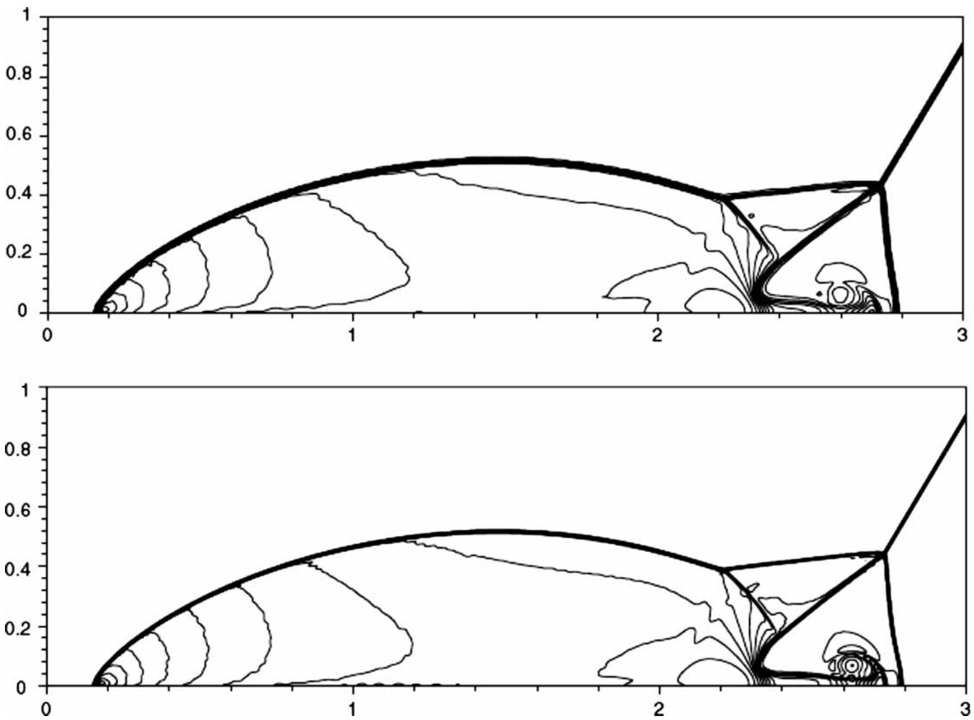

Figure 7. Double Mach reflection test problem, meshes of 480 × 120 (top), 960 × 240 (bottom) cells are used. A number of 30 contour lines from 2 to 22 are displayed.

4.1 Double mach reflection problem

The governing equation for this problem is the two-dimensional Euler equations (4.1). The computational domain is $[0,4] \times [0,1]$. The reflecting wall lies at the bottom of the computational domain starting from $x = (1/6)$. Initially a right moving Mach 10 shock is positioned at $(x, y) = ((1/6), 0)$ and makes a 60° angle with the x-axis. For the bottom boundary, the exact post-shock condition is imposed from $x = 0$ to $x = (1/6)$ and a reflective boundary condition is used for the rest of the x-axis. At the top boundary of the computational domain, the data is set to describe the exact motion of the Mach 10 shock; consult (Woodward and Colella 1984) for a detailed discussion of this problem.

Figure 7 shows the computed density by our scheme on the 480 × 120 and 960 × 240 cells. We observe that the scheme produces the flow pattern generally accepted in the present literature (Woodward and Colella 1984) as correct. All discontinuities are well resolved and correctly positioned.

References

Balagur, A. and Conde, C., Fourth order non-oscillatory upwind and central schemes for hyperbolic conservation laws. *SIAM J. Numer. Anal. V.*, 2005, **43**(2), 455–473.

Balsara, D.S. and Shu, C.W., Monotonicity preserving weighted essentially non-oscillatory schemes with increasingly high order of accuracy. *J. Comput. Phys.*, 2000, **160**, 405–452.

Glaiter, P., An approximate linearized Riemann solver for Euler equations for real gases. *J. Comp. Phys.*, 1988, **74**, 382–408.

Gottlieb, S., Shu, C.-W. and Tadmor, E., Strong stability-preserving high order time discretization methods. *SIAM Rev.*, 2001, **43**, 89–112.

Harten, A., Engquist, B., Osher, S. and Chakravarthy, S., Uniformly high order accurate essentially non-oscillatory schemes III. *J. Comp. Phys.*, 1987, **71**, 231–303.

Jiang, G.-S. and Shu, C.-W., Efficient implementation of weighted ENO schemes. *J. Comp. Phys.*, 1996, **126**, 202–228.

Kurganov, A. and Levy, D., A Third-order semi-discrete central scheme for conservation laws and convection–diffusion equations. *SIAM J. Sci. Comp.*, 2000, **22**, 1461–1488.

Kurganov, A. and Petrova, G., A Third-order semi-discrete genuinely multidimensional central scheme for hyperbolic conservation laws and related problems. *Numer. Math.*, 2001, **88**, 683–729.

Kurganov, A. and Tadmor, E., New high-resolution central schemes for nonlinear conservation laws and convection–diffusion equations. *J. Comp. Phys.*, 2000, **160**, 241–282.

Kurganov, A., Noelle, S. and Petrova, G., Semi-discrete central-upwind schemes for hyperbolic conservation laws and Hamilton–Jacobi equations. *SIAM J. Sci. Comp.*, 2001, **23**, 707–740.

Nessyahu, H. and Tadmor, E., Non-oscillatory central differencing for hyperbolic conservation laws. *J. Comp. Phys.*, 1990, **87**, 408–463.

Qiu, J. and Shu, C-W., On the construction, comparison, and local characteristic decomposition for the high order central WENO schemes. *J. Comput. Phys.*, 2002, **183**, 187–209.

Sod, G., A survey of several finite difference methods for systems of nonlinear hyperbolic conservation laws. *J. Comp. Phys.*, 1987, **27**, 1–31.

Woodward, P. and Colella, P., The numerical solution of two dimensional fluid flow with strong waves. *J. Comput. Phys.*, 1984, **54**, 115–173.